Chapter 5
Lubricated Joints for Mechanical Systems

In most machines and mechanisms, the joints are designed to operate with some lubricant fluid. The high pressures generated in the lubricant fluid act to keep the journal and the bearing apart. Moreover the thin film formed by lubricant reduces friction and wear, provides load-carrying capacity and adds damping to dissipate undesirable mechanical vibrations (Hamrock 1994, Frêne et al. 1997). Therefore the proper description of lubricated revolute joints, the so-called journal–bearings, in multibody systems is required to achieve better models and hence an improved understanding of the dynamic performance of machines. This aspect gains paramount importance due to the demand for the proper design of journal–bearings in many industrial applications (Ravn 1998, Bauchau and Rodriguez 2002). In the dynamic analysis of journal–bearings, the hydrodynamic forces, which include both squeeze and wedge effects, generated by the lubricant fluid, oppose the journal motion. It should be mentioned that the methodology presented here uses the superposition principle for load capacity due to the wedge effect entrainment and squeeze-film effect separately (Hamrock 1994). The hydrodynamic forces are obtained by integrating the pressure distribution evaluated with the aid of Reynolds' equation written for the dynamic regime (Pinkus and Sternlicht 1961). The hydrodynamic forces are nonlinear functions of the journal center position and of its velocity with reference to the bearing center. In the dynamic regime of a journal–bearing, the journal center has an orbit situated within a circle radius which is equal to the radial clearance. Thus a lubricated revolute joint does not impose kinematic constraints like an ideal revolute joint but instead it deals with force constraints as for the dry clearance joints. In a simple way, the hydrodynamic forces built up by the lubricant fluid are evaluated from the state of variable of the system and included into the equations of motion of the mechanical system (Nikravesh 1988). For dynamically loaded journal–bearings the classic analysis problem consists in predicting the motion of the journal center under arbitrary and known loading (Boker 1965, Goenka 1984). However, in the present work the time variable parameters are known from the dynamic system's configuration and the instantaneous force on the journal–bearing are evaluated afterwards.

In this chapter, a general methodology for modeling lubricated revolute joints in multibody mechanical systems is presented and discussed. A simple journal–bearing

P. Flores et al., *Kinematics and Dynamics of Multibody Systems with Imperfect Joints.*

subjected to a constant and unidirectional external load and a simple planar slider–crank mechanism, in which a lubricated revolute joint in the gudgeon-pin exists, are used as numerical applications in order to demonstrate the assumptions and procedures adopted.

5.1 General Issues in Tribology

In physical joints, clearance, friction and impact are always present, mainly when there is no fluid lubricant. These phenomena can significantly change the dynamic response of the mechanical systems in so far as the impact causes noise, increases the level of vibrations, reduces the fatigue life of the components and results in loss of precision. When the clearance joints are dry, i.e., without lubricant, contact and friction forces are the only effects present, representing the physical contact detected between the surfaces (Flores and Ambrósio 2004). However, in most the mechanical systems, the joints are designed to operate with some lubricant fluid. It is known that the use of lubricant in revolute joints is an effective way of ensuring better performance of the mechanical systems. In fact, lubricants are widely used in thin fluid film journal–bearing elements to reduce friction and wear, provide load capacity and add damping to dissipate undesirable mechanical vibrations.

Journal–bearing is a circular shaft, designated as journal, rotating in a circular bush, designated as bearing. The space between the two elements is filled with a lubricant. Under an applied load, the journal center is displaced from the bearing center and the lubricant is forced into the convergence clearance space causing a build-up of pressure. The high pressures generated in the lubricant film act to keep the journal and the bearing surfaces apart. It is well known from fluid mechanics that a necessary condition to develop pressure in a thin film is that the gradient and the slope of the velocity profile vary across the thickness of the film (Frêne et al. 1997).

Shown in Fig. 5.1 is the basic journal–bearing geometry. The length of the bearing is L and it has a diameter D. The difference between the radii of the bearing and the journal is the radial clearance c ($c = R_B\text{-}R_J$). In general, both the journal and the bearing may rotate nonuniformly, and the applied load may vary in both magnitude and direction.

In the region of the local converging film thickness, the hydrodynamic pressure rises to a maximum value and then decreases to ambient values at the side and trailing edges of the thin film. In zones where the film thickness locally increases, the fluid pressure may drop to ambient or below its vapor pressure leading to the release of dissolved gases within the lubricant vaporization causing film rupture. The phenomenon of film rupture is known as lubricant cavitation, and the effects on the performance and stability of journal–bearings are reasonably well understood and documented in the literature (Dowson and Taylor 1979, Elrod 1981, Woods and Brewe 1989, Mistry et al. 1997). The performance of journal–bearings considering lubricant supply conditions has been studied theoretically and experimentally by Miranda (1983), Claro (1994) and Costa (2000).

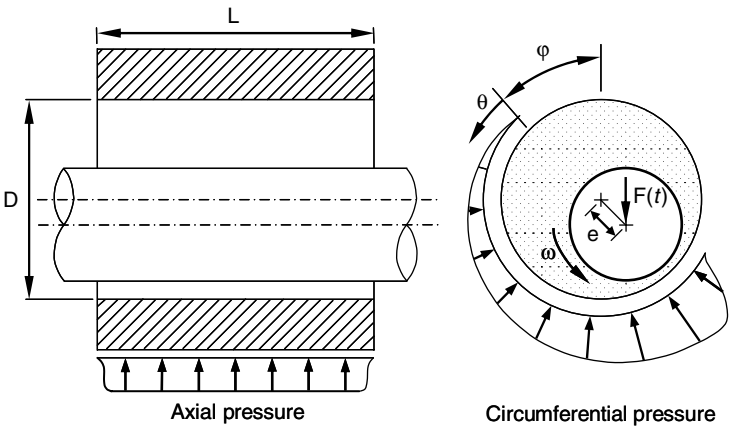

Fig. 5.1 Basic journal–bearing geometry

Journal–bearings are used in many important operating situations, in which the loads vary in both magnitude and direction, often cyclically. Examples include reciprocating machinery such as internal combustion engines, compressors, out of balance rotating machinery such as turbine rotors and other industrial processing machinery. The hydrodynamic fluid film developed in the journal–bearings exhibits damping which plays a very important role in the stability of the mechanical elements. In order to study the performance of such journal–bearings, it is necessary to determine the loads and their variation with time. In dynamically loaded journal–bearings, the eccentricity and the attitude angle vary through the loading cycle, and special care must be taken to ensure that the combination of load and speed rotation does not lead to a dangerous small minimum film thickness.

Lubricated joints are designed so that even when the maximum load is applied, the journal and bearing do not come in contact. One of the main reasons for designing journal–bearings in this way is to reduce friction and extend their lifetime. Consequently proper modeling of lubricated revolute joints in multibody mechanical systems is required to achieve a better understanding of the dynamic performance of the machines. This aspect plays a crucial role owing to the demand for proper design of the journal–bearings in many industrial applications.

5.2 Dynamic Characteristics of Journal–Bearings

If the journal and bearing have relative angular velocities with respect to each other, the amount of eccentricity adjusts itself until the pressure generated in the converging lubricating film balances the external loads. The pressure generated, and hence the load capacity of the journal–bearing, depends on the journal eccentricity, the relative angular velocity, the effective viscosity of the fluid lubricant and the journal–bearing geometry and clearance. There are two different actions of pressure

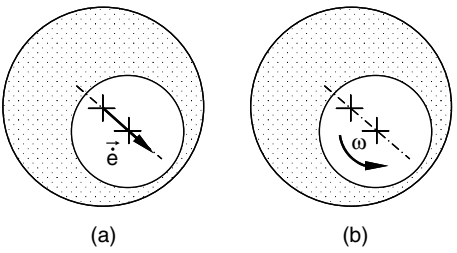

Fig. 5.2 (**a**) Squeeze-film action; (**b**) wedge-film action

generation in journal–bearings, namely wedge and squeeze actions, as shown in Fig. 5.2. The squeeze action relates the radial journal motion to the generation of load capacity pressure in the lubricant film, whilst the wedge action deals with the relation between relative rotational velocity of the journal and bearing ability to produce such pressure.

When only the squeeze action of the lubricant is considered, assuming a null or low relative rotational velocity and, hence, absence of relative tangential velocity, the journal load and the fluid reaction force are considered to have the same line of action, which is collinear with the center lines. However, in the more general case, in the presence of high angular velocities, they do not have the same line of action because of the wedge effect. When relative angular velocities are large, the simple squeeze approach is not valid and the general Reynolds' equation has to be used (Hamrock 1994, Frêne et al. 1997).

In general, mechanical systems demand journal–bearings in which the load varies in both magnitude and direction, which results in dynamically loaded journal–bearings. Figure 5.3 shows the cross-section of a smooth dynamically loaded journal–bearing. When the load acting on the journal–bearing is not constant in direction and/or module, the journal center describes an orbit within the bearing boundaries. Typical examples of dynamically loaded journal–bearings include

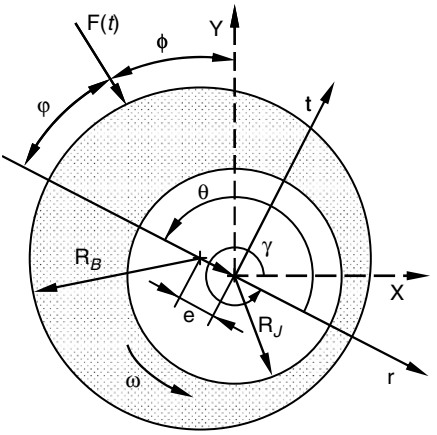

Fig. 5.3 Cross-section of a smooth dynamically loaded journal–bearing

the crankshaft bearings in combustion engines and high-speed turbine bearings supporting dynamic loads caused by unbalanced rotors.

In mechanical systems, a lubricated revolute joint does not produce any kinematic constraint. Instead it acts in a similar way to a force element producing time-dependent forces. Thus it deals with the so-called force constraints. For dynamically loaded journal–bearings the classic tribology analysis problem consists in predicting the motion of the journal center under arbitrary and known loads, using, for instance, the mobility method (Boker 1965, Goenka 1984). Conversely, in the work now presented, the time-variable parameters are known from the dynamic analysis and the instantaneous forces on the journal–bearing are calculated. In a simple way, the forces built up by the lubricant fluid are evaluated from the state of variables of the system and included into the equations of motion of the mechanical system as external generalized forces.

5.3 Hydrodynamic Forces in Dynamic Journal–Bearings

Theory of lubrication for dynamically loaded journal–bearings is mathematically complex, and the solution of the governing differential equations is based on many simplifying premises. The main basic principles, terminology and theoretical background are well discussed in the thematic literature, such as Hamrock (1994), Frêne et al. (1997), amongst others. Pinkus and Sternlicht (1961) present a detailed derivation of the Reynolds' equation, in which the forces developed by the fluid film pressure field are evaluated. The Reynolds' equation contains viscosity, density and film thickness as parameters. The full general form of the isothermal Reynolds' equation for a dynamically loaded journal–bearing is written as

$$\frac{\partial}{\partial X}\left(\frac{h^3}{\mu}\frac{\partial p}{\partial X}\right)+\frac{\partial}{\partial Z}\left(\frac{h^3}{\mu}\frac{\partial p}{\partial Z}\right)=6U\frac{\partial h}{\partial X}+12\frac{dh}{dt} \tag{5.1}$$

where X is the radial direction, Z is the axial direction, μ is the dynamic fluid viscosity, h denotes the film thickness and p is the pressure. The two terms on the right-hand side of (5.1) represent the two different effects of pressure generation on the lubricant film, i.e., wedge and squeeze actions, respectively.

It is known that (5.1) is a nonhomogeneous partial differential of the elliptical type. The exact solution of the Reynolds' equation is difficult to obtain and, in general, requires a considerable numerical effort. However, it is possible to solve the equation analytically by setting to zero either the first or second term on the left-hand side. These solutions correspond to those for infinitely short and infinitely long journal–bearings, respectively.

Dubois and Ocvirk (1953) consider a journal–bearing where the pressure gradient around the circumference is very small when compared with those along the length. This assumption is valid for length-to-diameter (L/D) ratios up to 0.5. Hence the Reynolds' equation for an infinitely short journal–bearing can be written as

$$\frac{\partial}{\partial Z}\left(\frac{h^3}{\mu}\frac{\partial p}{\partial Z}\right) = 6U\frac{\partial h}{\partial X} + 12\frac{dh}{dt} \tag{5.2}$$

When the relative pressure is zero at journal–bearing ends the pressure in the fluid film is given by (Frêne et al. 1997)

$$p(\theta, Z) = -\frac{3\mu}{h^3}\left(\frac{L^2}{4} - Z^2\right)\left((\omega - 2\dot{\gamma})\frac{\partial h}{\partial \theta} + 2\dot{e}\cos\theta\right) \tag{5.3}$$

where θ is the angular coordinate, Z is the axial direction, L represents the journal–bearing length, μ is the dynamic fluid viscosity, h denotes the film thickness and ω is the relative angular velocity between the journal and bearing. The dot in the above expression denotes the time derivative of the corresponding parameter.

For an infinitely long journal–bearing a constant fluid pressure and negligible leakage in the axial direction are assumed. In many cases, it is possible to treat a journal–bearing as infinitely long and consider only its middle point. This solution was first derived by Sommerfeld (1904) and is valid for length-to-diameter (L/D) ratios greater than 2. Thus the Reynolds' equation for an infinitely long journal–bearing is

$$\frac{\partial}{\partial X}\left(\frac{h^3}{\mu}\frac{\partial p}{\partial X}\right) = 6U\frac{\partial h}{\partial X} + 12\frac{dh}{dt} \tag{5.4}$$

And the pressure distribution in the fluid is given by (Frêne et al. 1997)

$$p = 6\mu\left(\frac{R_J}{c}\right)^2\left\{\frac{(\omega - 2\dot{\gamma})(2 + \varepsilon cos\theta)\varepsilon sin\theta}{(2+\varepsilon^2)(1+\varepsilon cos\theta)^2} + \frac{\dot{\varepsilon}}{\varepsilon}\left[\frac{1}{(1+\varepsilon cos\theta)^2} - \frac{1}{(1+\varepsilon)^2}\right]\right\} \tag{5.5}$$

where R_J is the journal radius, c is the radial clearance and ε is the eccentricity ratio.

It is convenient to determine the force components of the resultant pressure in directions tangential and perpendicular to the line of centers. These force components can be obtained by integrating the pressure field either in the entire domain 2π or half-domain π. In the later case, the pressure field is integrated only over the positive part by setting the pressure in the remaining portion equal to zero. These boundary conditions, associated with the pressure field, correspond to Sommerfeld's and Gümbel's boundary conditions (Fig. 5.4).

The Sommerfeld's boundary conditions, complete or full film, do not take into account the cavitation phenomenon and, consequently, contemplate the existence of negative pressures for the region $\pi<\theta<2\pi$. This case is not realised in many applications due to the fluid incapacity to sustain significant sub-ambient pressures.

The Gümbel's conditions, which account for the rupture film, assume the existence of a zero pressure zone for the region between π and 2π. Though the Gümbel's, or half Sommerfeld's solution, results in more realistic predictions of

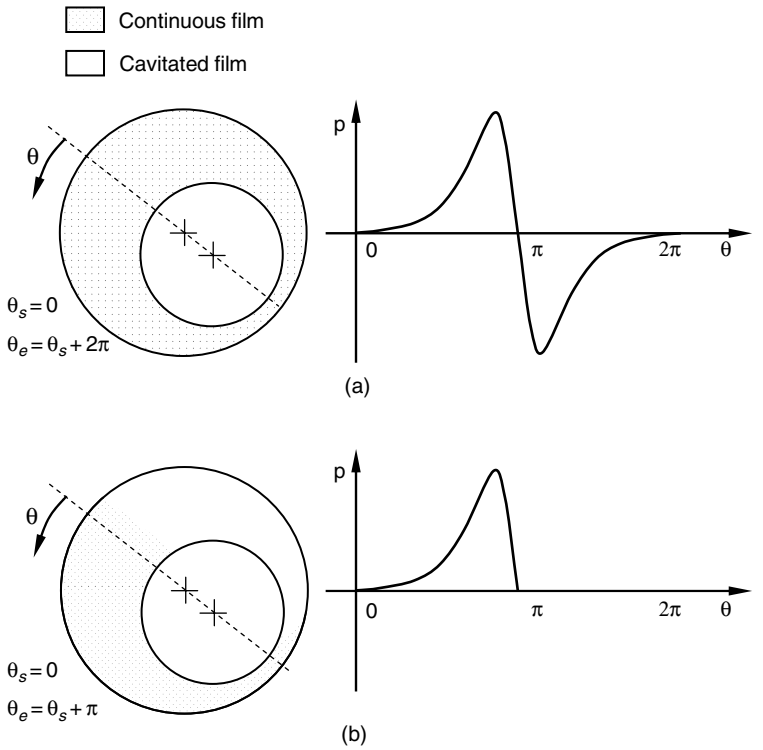

Fig. 5.4 (**a**) Sommerfeld's boundary conditions; (**b**) Gümbel's boundary conditions

the load capacity, it leads to a violation of the continuity of flow at the outlet end of the pressure curve.

For the Sommerfeld's conditions, i.e., full film, the force components of the fluid film for infinitely short journal–bearing are written as (Frêne et al. 1997)

$$F_r = -\frac{\pi\mu L^3 R_J}{c^2}\frac{\dot{\varepsilon}(1+2\varepsilon^2)}{(1-\varepsilon^2)^{5/2}} \tag{5.6}$$

$$F_t = \frac{\pi\mu L^3 R_J}{c^2}\frac{\varepsilon(\omega-2\dot{\gamma})}{2(1-\varepsilon^2)^{3/2}} \tag{5.7}$$

where F_r is the radial component of the force while F_t is the tangential component, as Fig. 5.3 shows.

For the Gümbel's conditions, i.e., rupture film, the force components of the fluid film for infinitely short journal–bearing can be expressed as (Frêne et al. 1997)

$$F_r = -\frac{\mu L^3 R_J}{2c^2(1-\varepsilon^2)^2}\left(\frac{\pi\dot{\varepsilon}(1+2\varepsilon^2)}{(1-\varepsilon^2)^{1/2}} + 2\varepsilon^2(\omega - 2\dot{\gamma})\right) \tag{5.8}$$

$$F_t = \frac{\mu L^3 R_J \varepsilon}{2c^2(1-\varepsilon^2)^2}\left(4\dot{\varepsilon} + \frac{\pi}{2}(\omega - 2\dot{\gamma})\sqrt{1-\varepsilon^2}\right) \tag{5.9}$$

As for the case of the infinitely short journal–bearing, the complete film and the film rupture for the infinitely long journal–bearing are also distinguished. Thus, for the Sommerfeld's conditions, full film, the force components of the fluid film for infinitely long journal–bearing are written as (Frêne et al. 1997)

$$F_r = -\frac{12\pi\mu L R_J^3 \dot{\varepsilon}}{c^2(1-\varepsilon^2)^{3/2}} \tag{5.10}$$

$$F_t = \frac{12\pi\mu L R_J^3 \varepsilon(\omega - 2\dot{\gamma})}{c^2(2+\varepsilon^2)(1-\varepsilon^2)^{1/2}} \tag{5.11}$$

For the Gümbel's conditions the force components of the fluid film for infinitely long journal–bearing are written as (Frêne et al. 1997)

$$F_r = -\frac{12\mu L R_J^3}{c^2}\left(\frac{\varepsilon^2(\omega - 2\dot{\gamma})}{(2+\varepsilon^2)(1-\varepsilon^2)} + \frac{\dot{\varepsilon}}{(1-\varepsilon^2)^{3/2}}\left(\frac{\pi}{2} - \frac{8}{\pi(2+\varepsilon^2)}\right)\right) \tag{5.12}$$

$$F_t = \frac{12\mu L R_J^3}{c^2}\left(\frac{\pi\varepsilon(\omega - 2\dot{\gamma})}{2(2+\varepsilon^2)\sqrt{1-\varepsilon^2}} + \frac{2\varepsilon\dot{\varepsilon}}{(2+\varepsilon^2)(1-\varepsilon^2)}\right) \tag{5.13}$$

In fact, the main difficulty in obtaining satisfactory solutions of journal–bearing performance lies not only in solving the differential equations but also in defining adequately the boundary conditions of Reynolds' equation. In dynamically loaded journal–bearings, obtaining the force components from the integration of the Reynolds' equation only over the positive pressure regions, by setting the pressure in the remaining portions equal to zero, involves finding the zero points, i.e., the angles θ_s at which the pressure begins and θ_e when it ends. For the case of a steady-state journal–bearing, these angles are, in general, assumed to be equal to 0 and π, respectively. However, for a dynamically loaded journal–bearing these angles are time-dependent and the evaluation of the force components involves a good deal of mathematical manipulation. For details in their treatment see the work by Pinkus and Sternlicht (1961). The hydrodynamic force components, along the eccentricity direction and normal to it, are for radial velocity greater than zero, $\dot{\varepsilon} > 0$, given by Pinkus and Sternlicht (1961) as

$$F_r = -\frac{\mu L R_J^3}{c^2} \frac{6\dot{\varepsilon}}{(2+\varepsilon^2)(1-\varepsilon^2)^{3/2}} \left[4k\varepsilon^2 + (2+\varepsilon^2)\pi \frac{k+3}{k+3/2} \right] \tag{5.14}$$

$$F_t = \frac{\mu L R_J^3}{c^2} \frac{6\pi\varepsilon(\omega - 2\dot{\gamma})}{(2+\varepsilon^2)(1-\varepsilon^2)^{1/2}} \frac{k+3}{k+3/2} \tag{5.15}$$

For a negative radial velocity $\dot{\varepsilon} < 0$, the force components are written as follows:

$$F_r = -\frac{\mu L R_J^3}{c^2} \frac{6\dot{\varepsilon}}{(2+\varepsilon^2)(1-\varepsilon^2)^{3/2}} \left[4k\varepsilon^2 - (2+\varepsilon^2)\pi \frac{k}{k+3/2} \right] \tag{5.16}$$

$$F_t = \frac{\mu L R_J^3}{c^2} \frac{6\pi\varepsilon(\omega - 2\dot{\gamma})}{(2+\varepsilon^2)(1-\varepsilon^2)^{1/2}} \frac{k}{k+3/2} \tag{5.17}$$

where the parameter k is defined as

$$k^2 = (1-\varepsilon^2) \left[\left(\frac{\omega - 2\dot{\gamma}}{2\dot{\varepsilon}} \right)^2 + \frac{1}{\varepsilon^2} \right] \tag{5.18}$$

Finally the force components of the resulting pressure distribution, tangential and perpendicular to the line of centers, have to be projected onto the X and Y directions. From Fig. 5.3 it is clear that

$$F_x = F_r cos\gamma - F_t sin\gamma \tag{5.19}$$

$$F_y = F_r sin\gamma + F_t cos\gamma \tag{5.20}$$

Equations (5.6)–(5.18), for infinitely short and infinitely long journal–bearings, present the relation between the journal center motion and the fluid reaction force on the journal. The solution of these equations presents no problem since the journal center motion is known from the dynamic analysis of the mechanical system.

In traditional tribology analysis of journal–bearings, the external forces are known and the motion of the journal center inside the bearing boundaries is evaluated by solving the differential equations for the time-dependent variables. However, in the present work instead of knowing the applied load, the relative journal–bearing motion characteristics are known. Afterwards the fluid force, from the pressure distribution in the lubricant, is calculated. Thus, since all the states of variables are known from dynamic analysis of the mechanical system, the hydrodynamic forces given by (5.19) and (5.20) can be evaluated and introduced as external generalized forces into the system's equations of motion of the multibody mechanical system.

5.4 Transition Between Hydrodynamic and Dry Contact

In this section, a transition model, which combines the squeeze action and the dry contact model, is discussed. This model that considers the existence of lubrication during the free flight trajectory of the journal, prior to contact, and the possibility for dry contact under some conditions, seems to be well fitted to describe revolute joints with clearances in mechanical systems.

In what follows, the expression for the squeeze forces of infinite long journal–bearings is presented. The objective is to evaluate the resulting force from the given state of position and velocity of the journal–bearing. The squeeze forces are exerted when a fluid is squeezed between two approaching surfaces. In journal–bearings, squeeze action is dominant when the relative angular velocity is small compared to the relative radial velocity and, hence, it is reasonable to drop the wedge term in the Reynolds' equation.

In the infinitely long journal–bearing the axial flow is neglected when compared with the circumferential flow, hence the Reynolds' equation reduces to a one-dimensional problem and the pressure field is given by (Hamrock 1994)

$$p = \frac{6\mu R_J^3 \dot{\varepsilon}}{c^2} \frac{cos\theta(2 - \varepsilon cos\theta)}{(1 - \varepsilon cos\theta)^2} \tag{5.21}$$

The resulting force F on the journal that balances the fluid pressure is evaluated as an integral of the pressure field over the surface of the journal:

$$F = \frac{12\pi\mu L R_J^3 \dot{\varepsilon}}{c^2(1 - \varepsilon^2)^{\frac{3}{2}}} \tag{5.22}$$

where μ is the dynamic lubricant viscosity, L is the journal–bearing length, R_J is the journal radius, c is the radial clearance, ε is the eccentricity ratio and $\dot{\varepsilon}$ is the time rate of change of eccentricity ratio.

The direction of the force is along the line of centers that connects the journal and the bearing, which is described by the eccentricity vector. Thus the squeeze force can be introduced into the equations of motion of multibody mechanical systems as a generalized force with the journal and bearing centers as points of action for the force and reaction force, respectively. It should be highlighted that the effect of cavitation is not considered in (5.22), that is, it is assumed that a continuous film exists all around the journal–bearing. However, these conditions are not satisfactory from the physical point of view because the lubricant fluids cannot sustain negative pressures. Based on the mechanics of the journal–bearing, Ravn et al. (2000) included a cavitation effect assuming that negative pressure occurs on the half of journal surface which faces away from the moving direction.

Equation (5.22), which represents the action on the journal that maintains in equilibrium the field pressure, is valid for situations when the load capacity of the wedge effect is negligible when compared to that of the squeeze effect. In the squeeze lubrication, the journal moves along a radial line in the direction of the applied load,

thus the film thickness decreases and the fluid is forced to flow up around the journal and out from the ends of the bearing. Since the squeeze force is proportional to the rate of decrease of the fluid film thickness, it is apparent that the lubricant acts as a nonlinear viscous damper resisting the load when the film thickness is decreasing. As the fluid film thickness becomes very thin, that is, the journal is very close to the bearing surface, the force due to the lubricant evaluated from (5.22) becomes very large. Hence a discontinuity appears when the film thickness approaches zero and, consequently, the squeeze force tends to infinity.

For highly loaded contact, the pressure causes elastic deformation of the surfaces, which can be of the same order as the lubricant film thickness. These circumstances are dramatically different from those found in the hydrodynamic regime. The contribution of the theory of elasticity with the hydrodynamic lubrication is called elasto-hydrodynamic lubrication theory (EHL).

Figure 5.5 schematically shows the shape of the lubricant film thickness and the pressure distribution within a typical elasto-hydrodynamic contact. Due to the normal load F the contacting bodies are deformed. The viscous lubricant, adhering to the surfaces of the moving bodies, is dragged into the high-pressure zone of the contact and therefore separates the mating surfaces. The pressure distribution within the elasto-hydrodynamic contact is similar to the dry Hertzian pressure distribution. At the inlet zone, the pressure slowly builds up until it approximately reaches the maximum Hertzian pressure (p). It is, therefore, assumed that for a certain film thickness, called boundary layer, the fluid can no longer be squeezed and the journal and bearing walls are considered to be in contact, in a way similar to that for the dry contact situation presented in Chap. 4. It should be highlighted that the EHL theory is quite complex and its detailed description is beyond the scope of the present work. However, another equivalent model, based on physical reasoning, can be proposed leading to effects similar to those of the EHL theory.

A transition model which combines the squeeze action and the dry contact model is proposed here. Figure 5.6 shows a partial view of a mechanical system representing a revolute clearance joint with lubrication effect, where both the journal and the bearing can have planar motion. The parallel spring–damper element represented

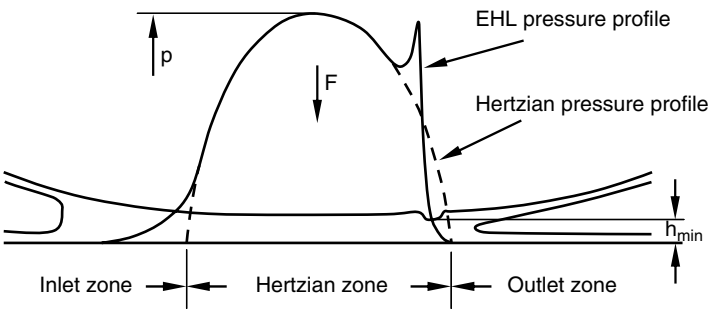

Fig. 5.5 Typical elasto-hydrodynamic contact; qualitative shape of lubricant film and pressure profile

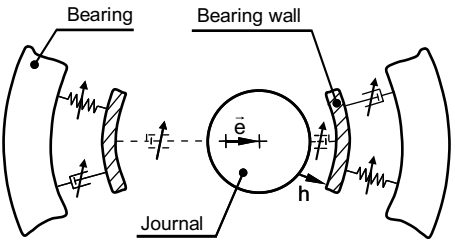

Fig. 5.6 Mechanical system representing a revolute joint with lubrication effect

by a continuous line refers to the solid-to-solid contact between the journal and the bearing wall, whereas the damper represented by a dashed line refers to the lubricated model. If there is no lubricant between the journal and the bearing, the journal can freely move inside the bearing boundaries. When the gap between the two elements is filled with a fluid lubricant, a viscous resistance force exists and opposes the journal motion. Since the radial clearance is specified, the journal and bearing can work in two different modes. In mode 1, the journal and the bearing wall are not in contact with each other and they have a relative radial motion. For the journal–bearing model without lubricant, when $e<c$ the journal is in free flight motion and the forces associated with the journal–bearing are set to zero. For lubricated journal–bearing model, the lubricant transmits a force, which must be evaluated from the state variables of the mechanical system using one of the models described in the previous section. In mode 2, the journal and the bearing wall are in contact, thus the contact force between the journal and the bearing is modeled with the continuous contact force model represented by (3.9).

Since the EHL pressure profile is similar to the Hertzian pressure distribution, it looks reasonable to change from the squeeze action in the hydrodynamic lubrication regime to the pure dry contact model. In order to avoid numerical instabilities and to ensure a smooth transition from pure squeeze model to dry contact model, a weighted average is used. When the journal reaches the boundary layer, for which the hydrodynamic theory is no longer valid, the squeeze force model is replaced by the dry contact force model, as represented in Fig. 5.7a and b. This approach ensures continuity in the joint reaction forces when the squeeze force model is switched to dry contact force model. Mathematically the transition force model is expressed by

$$F = \begin{cases} F_{squeeze} & \text{if} \quad e \le c \\ \dfrac{(c+e_{t0})-e}{e_{t0}} F_{squeeze} + \dfrac{e-c}{e_{t0}} F_{dry} & \text{if} \quad c \le e \le c+e_{t0} \\ F_{dry} & \text{if} \quad e \ge c+e_{t0} \end{cases} \tag{5.23}$$

where e_{t0} and e_{t1} are given tolerances for the eccentricity. The values of these parameters must be chosen carefully, since they depend on the clearance size. It should be noted that the clearance used for the pure squeeze force model is not c but it is $c + e_{t1}$ instead.

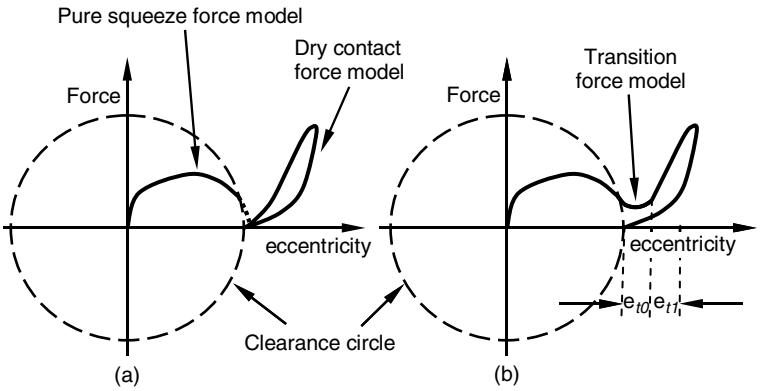

Fig. 5.7 (**a**) Pure squeeze and dry contact force models; (**b**) transition force model between lubricated and dry contact situations

5.5 Kinematic Aspects of the Journal–Bearing Interaction

In order to evaluate the forces produced by the fluid lubricant on the journal–bearing interface, the different dynamic parameters on which these forces depend need to be evaluated. It is clear that the hydrodynamic forces are nonlinear functions of the time parameters, ω, ε, $\dot{\varepsilon}$, γ and $\dot{\gamma}$, which are known at any instant of time from the dynamic system configuration, i.e., these parameters are functions of the system state variables.

Let Fig. 4.4 be redrawn here to highlight the existence of the lubricant fluid in the gap between the journal and the bearing. The two bodies i and j are connected by a lubricated revolute joint, in which the gap between the bearing and the journal is filled with a fluid lubricant. Part of body i is the bearing and part of body j is the journal. The notation used in Fig. 5.8 is the same described in Sect. 4.2.

The parameter ε, which defines the eccentricity ratio, is obtained as the ratio of the distance between the bearing and journal centers by radial clearance, that is,

$$\varepsilon = \frac{e}{c} \tag{5.24}$$

where the eccentricity e is given by (4.3).

The parameter $\dot{\varepsilon}$ can be obtained by differentiating (4.1), and dividing the result by the radial clearance. For the purpose let (4.1) be re-written as

$$\mathbf{e} = \mathbf{r}_j^P + \mathbf{A}_j \mathbf{s}'^P_j - \mathbf{r}_i^P - \mathbf{A}_i \mathbf{s}'^P_i \tag{5.25}$$

then its time derivative is

$$\dot{\mathbf{e}} = \dot{\mathbf{r}}_j^P + \dot{\mathbf{A}}_j \mathbf{s}'^P_j - \dot{\mathbf{r}}_i^P - \dot{\mathbf{A}}_i \mathbf{s}'^P_i \tag{5.26}$$

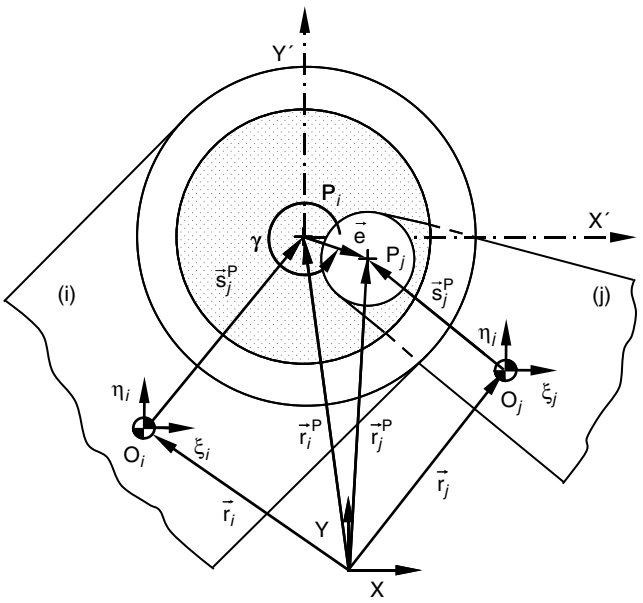

Fig. 5.8 Generic configuration of a dynamically loaded journal–bearing in a multibody mechanical system

Hence the time rate of eccentricity ratio is given by

$$\dot{\varepsilon} = \frac{\dot{e}}{c} \tag{5.27}$$

The line of centers between the bearing and the journal makes an angle γ with X′-axis as shown in Fig. 5.8. Since the unit radial vector **n** has the same direction as the line of centers, the angle γ can be defined as

$$\begin{bmatrix} cos\ \gamma \\ sin\ \gamma \end{bmatrix} = \begin{bmatrix} n_x \\ n_y \end{bmatrix} \tag{5.28}$$

Thus

$$\gamma = tan^{-1} \frac{n_y}{n_x} \tag{5.29}$$

The parameter $\dot{\gamma}$ can be obtained by differentiating (5.29) with respect to time, yielding

$$\dot{\gamma} = \frac{e_x \dot{e}_y - \dot{e}_x e_y}{e^2} \tag{5.30}$$

The hydrodynamic components of force resulting from pressure field projected onto the X and Y directions given by (5.19) and (5.20) act on the journal center.

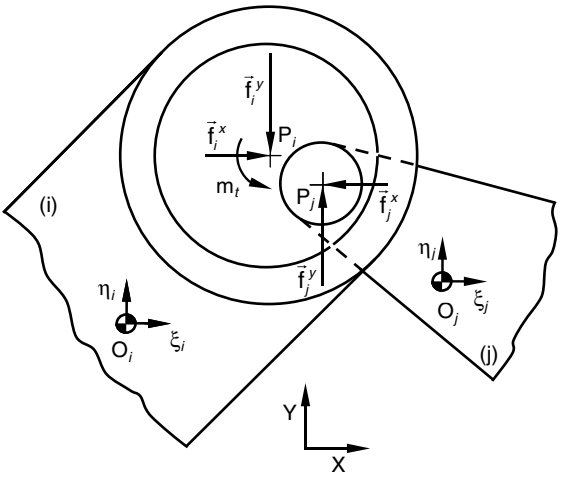

Fig. 5.9 Vectors of forces that act on the journal and bearing

Thus these forces have to be transferred to the centers of mass of the bearing and the journal bodies. From Fig. 5.9, the forces and moments that act on the center of mass of journal body are given by

$$\begin{bmatrix} f_j^x \\ f_j^y \\ m_j \end{bmatrix} = \begin{bmatrix} F_x \\ F_y \\ -(\xi_j^P sin\varphi_j + \eta_j^P cos\varphi_j)F_x + (\xi_j^P cos\varphi_j - \eta_j^P sin\varphi_j)F_y \end{bmatrix} \tag{5.31}$$

and for the center of mass of bearing body, at point O_i,

$$\begin{bmatrix} f_i^x \\ f_i^y \\ m_i \end{bmatrix} = \begin{bmatrix} -F_x \\ -F_y \\ (\xi_i^P sin\varphi_i + \eta_i^P cos\varphi_i + e_y)F_x - (\xi_i^P cos\varphi_i - \eta_i^P sin\varphi_i + e_x)F_y \end{bmatrix} \tag{5.32}$$

The transport moment produced by transferring the forces from the center of journal to the center of the bearing is given by $m_t = e_y F_x - e_x F_y$, which is already included in the force vector given by (5.32).

5.6 Application Example 1: Simple Journal–Bearing

In this section, as an application example, a simple journal–bearing subjected to a constant and unidirectional external load is considered, as shown in Fig. 5.10. The journal–bearing under constant unidirectional load contains both the dynamic characteristics within the transient period and the steady hydrodynamic characteristics within the steady-state period.

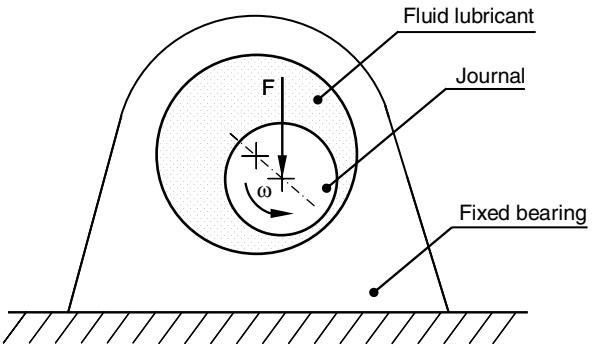

Fig. 5.10 Simple journal–bearing subjected to a constant external load

The journal–bearing properties and initial conditions are listed in Table 5.1. Initially the journal and bearing centers coincide. The oil fluid used in the present example is a SAE 40 multigrade, which is recommended for small combustion engines, and at 40°C the viscosity is equal to 400 cP. In order to analyze the performance of the models proposed, the simple journal–bearing performance is described by the journal center trajectory inside the bearing boundaries, as represented in Fig. 5.11a–e, and by the horizontal and vertical component of the reaction fluid force, shown in Figs. 5.12 and 5.13, respectively.

For the hydrodynamic journal–bearing models that use the Sommerfeld's boundary conditions, the journal center oscillates around its equilibrium position, as observed in Fig. 5.11a and c, whereas for the Gümbel's conditions, after an initial overshoot and transient period, the journal reaches its final equilibrium position, displayed in Fig. 5.11b and d. In the equilibrium position, the squeeze effect becomes null, that is, $\dot{\varepsilon} = 0$. Hence the forces generated by the wedge action balances the external applied load, which in this particular situation is $F_X = 0$, as observed in Fig. 5.12b and d, and $F_Y = F$, as shown in Fig. 5.13b and d. This is expected since the steady-state position is reached and the journal rotates about its whirl. When the Pinkus and Sternlicht hydrodynamic model is used, the journal also reaches the final equilibrium position but with lower damping, as shown in Figs. 5.11e, 5.12e and 5.13e. Indeed this model predicts lower damping and higher fluctuations in the transient phase which seems to be more realistic since in practical cases the oscillation and instability of the journal–bearing are among the main concerns of any analysis. The overall results are corroborated by published works about this field (Alshaer and Lankarani 2001).

Table 5.1 Dynamic properties of the simple journal–bearing

External load	30 N	Journal mass	0.13 kg
Bearing radius	10.0 mm	Journal rotational inertia	2.5×10^{-4} kg m^2
Journal radius	9.8 mm	Journal angular speed	500 rpm
journal–bearing length	40.0 mm	Oil viscosity at 40°C	400 cP

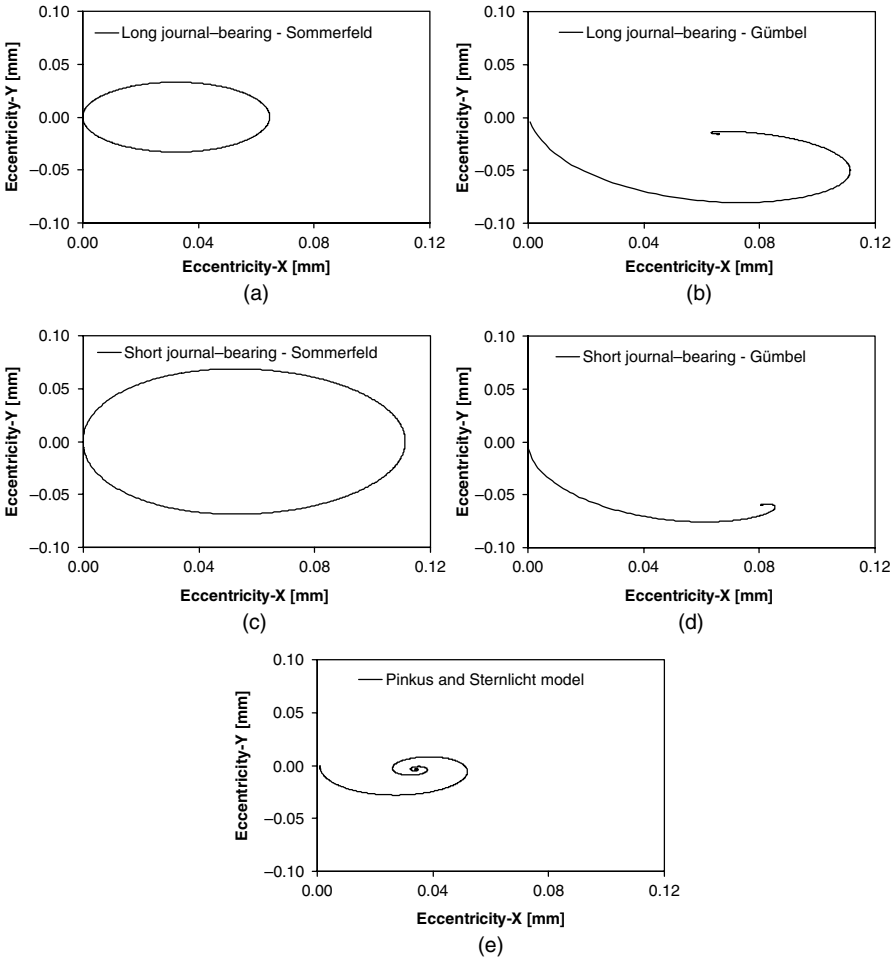

Fig. 5.11 Trajectory of the journal center inside the bearing boundaries for the different dynamically loaded journal–bearing models: (**a**) infinitely long journal–bearing with Sommerfeld's conditions; (**b**) infinitely long journal–bearing with Gümbel's conditions; (**c**) infinitely short journal–bearing with Sommerfeld's conditions; (**d**) infinitely short journal–bearing with Gümbel's conditions; (**e**) Pinkus and Sternlicht hydrodynamic model

When observing the results, it should be pointed out that from the physical point of view a simple journal–bearing subjected to a constant and unidirectional external load corresponds to the free vibration system. The journal is under the influence of a suddenly applied force, which means that the journal is pulled out from the position of stable equilibrium by a small amount and released. A closer look at the forces, displayed in Fig. 5.12, shows that in all models F_X converges or oscillates about $F_X = 0\,\text{N}$ while Fig. 5.13 shows that the trend is convergence or oscillation of F_Y about $F_X = 31.275\,\text{N}$.

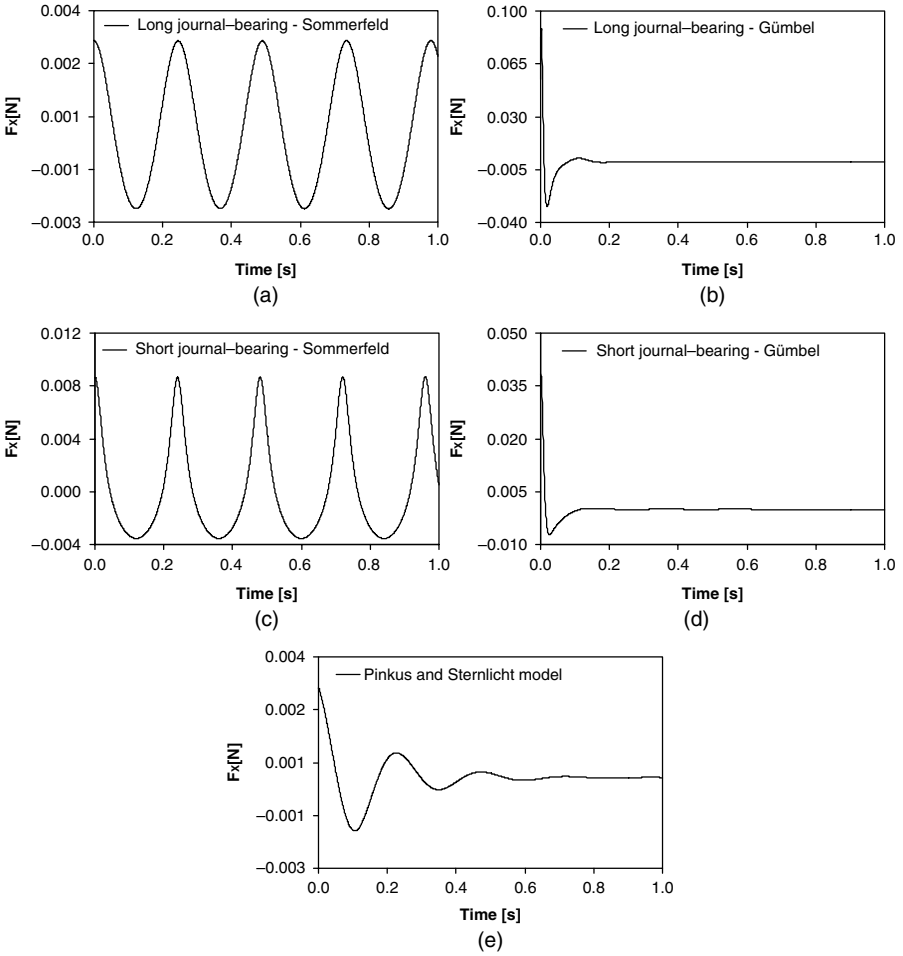

Fig. 5.12 Horizontal reaction force on the journal for the different dynamically loaded journal–bearing models: (**a**) infinitely long journal–bearing with Sommerfeld's conditions; (**b**) infinitely long journal–bearing with Gümbel's conditions; (**c**) infinitely short journal–bearing with Sommerfeld's conditions; (**d**) infinitely short journal–bearing with Gümbel's conditions; (**e**) Pinkus and Sternlicht hydrodynamic model

The journal–bearing performance for the hydrodynamic models with Sommerfeld's boundary conditions corresponds to a free vibration without damping, in which the journal is pulled out of its equilibrium position and then released without initial velocity and, consequently, the motion persists forever. The undamped free vibration, being periodic, is represented by a rotating vector, the end of which describes the circle observed in Fig. 5.11a and c. Yet the Gümbel's solutions, shown in Fig. 5.11b and d, and the Pinkus and Sternlicht model represent a damped free vibration system. In the later model the end point of the rotating vector describes the logarithmic spiral, displayed in Fig. 5.11e. The damped cycle path has its pole at the

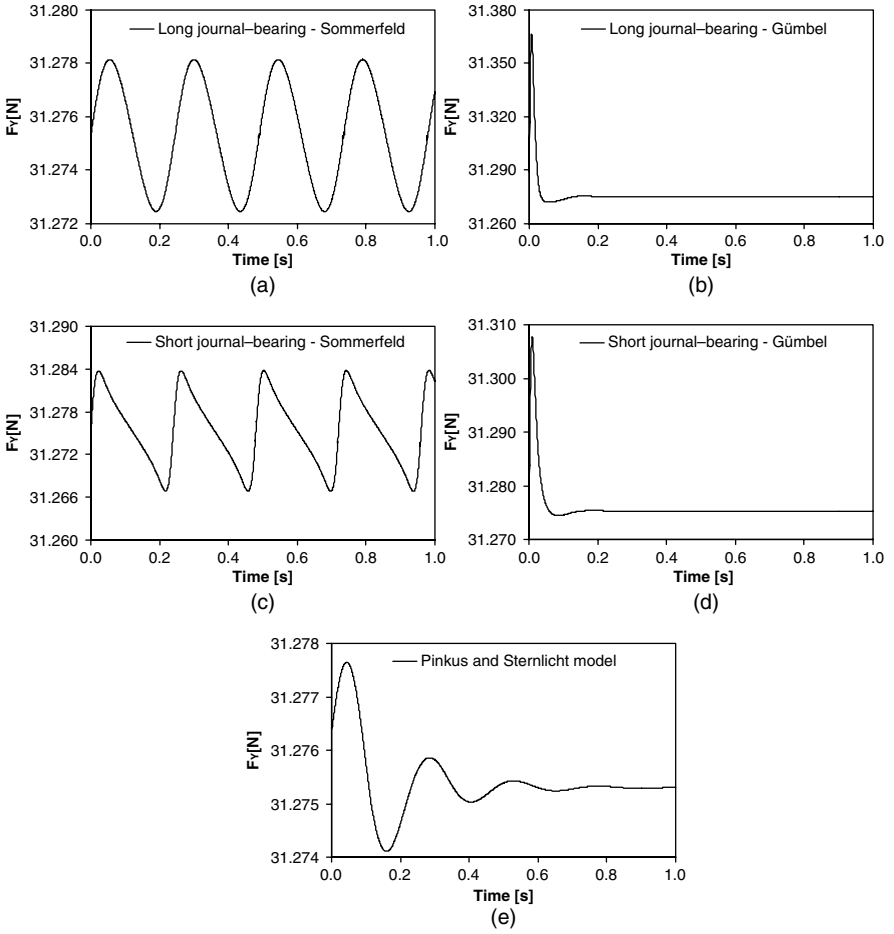

Fig. 5.13 Vertical reaction force on the journal for the dynamically loaded journal–bearing models: (**a**) infinitely long journal–bearing with Sommerfeld's conditions; (**b**) infinitely long journal–bearing with Gümbel's conditions; (**c**) infinitely short journal–bearing with Sommerfeld's conditions; (**d**) infinitely short journal–bearing with Gümbel's conditions; (**e**) Pinkus and Sternlicht hydrodynamic model

steady-state equilibrium position. In fact, the damped oscillations play an important role in the various forms of hydrodynamic instability and vibration, particularly in lightly loaded journal–bearings.

The final equilibrium position clearly depends on the applied load, physical and dynamic properties of the journal–bearing and the hydrodynamic model used. The steady-state equilibrium position does not occur in a dynamically loaded journal–bearing because the applied load varies in both magnitude and direction. This issue is discussed in the next section where a simple planar mechanical system with a dynamically loaded journal–bearing is considered.

5.7 Demonstrative Example 2: Slider–Crank Mechanism

The slider–crank mechanism used in the previous chapter is selected again here as an application example to study the influence of modeling the lubricated revolute joints in the dynamic behavior of mechanical systems. Figure 5.14 shows the configuration of the slider–crank model. The revolute joint between the connecting rod and slider is modeled as lubricated joint. Initially the journal and bearing centers coincide. The crank is the driving link and rotates with a constant angular velocity of 5000 rpm. Furthermore the initial conditions necessary to start the dynamic analysis are obtained from kinematic analysis of the mechanism in which all the joints are considered as ideal joints. The dynamic parameters used in the simulations are listed in Table 5.2.

In order to better understand the influence of the lubricated revolute joint models on the dynamic performance of the slider–crank mechanism, some of the results relative to the dry contact situation discussed in the previous chapter are presented again. Thus, in what follows, four different situations are analyzed and discussed. In the first one, the revolute joint is modeled as dry frictionless contact and the normal contact force law is given by Lankarani and Nikravesh model and expressed by (3.9). In the second case, besides this contact force model, the modified Coulomb friction law given by (3.16) is also included. In the third situation, the revolute clearance joint is modeled by using the transition model, that is, a combination between the dry contact force model and the pure squeeze force model presented in Sect. 5.4. In the fourth simulation the clearance revolute joint is modeled with the hydrodynamic Pinkus and Sternlicht model given by (5.14)–(5.18).

The dynamic behavior of the slider–crank mechanism simulations is quantified by plotting the values of the slider velocity and acceleration and the moment that acts on the crank, represented by Figs. 5.15–5.17. Additionally the journal center trajectories as well as the Poincaré maps are plotted in Figs. 5.18 and 5.19. The results are relative to two complete crank rotations after the transient effect has fadeout.

When observing the slider velocity, slider acceleration and crank moment diagrams, the influence of the joint clearance model is evident. For the cases of dry contact models with and without friction, displayed in Figs. 5.15a, b, 5.16a, b and 5.17a, b, high peaks on the acceleration and moment are visible, which means that

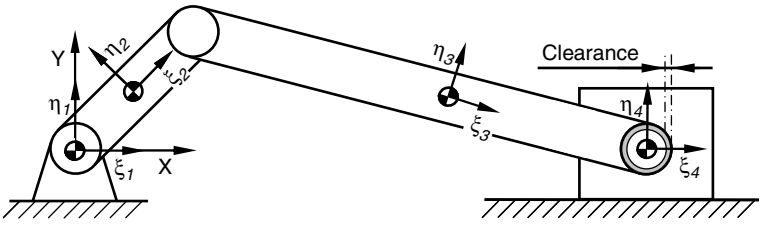

Fig. 5.14 Slider–crank mechanism with a lubricated revolute clearance joint

Table 5.2 Dynamic properties of the simple journal–bearing

Bearing radius	10.0 mm	Young's modulus	207 GPa
Journal radius	9.5 mm	Poisson's ratio	0.3
Journal–bearing length	40.0 mm	Baumgarte - α	5
Restitution coefficient	0.9	Baumgarte - β	5
Friction coefficient	0.03	Integration step size	0.00001 s
Oil viscosity at 40°C	400 cP	Integration tolerance	0.000001 s

the journal and bearing impact each other. Periods of continuous or permanent contact between the journal and bearing, shown in Figs. 5.18a and b, can also be observed. Furthermore the dynamic response of the slider–crank mechanism for dry contact model is clearly nonperiodic, as shown in the corresponding Poincaré maps, presented in Fig. 5.19a and b. However, when the friction effect is included, the peaks on the slider accelerations and, consequently, on the crank moments are reduced, as observed in Figs. 5.16b and 5.17b.

When the transition model is employed, the peaks on the slider acceleration and crank moment curves are smaller when compared to those obtained for dry contact models, as observed in Figs. 5.16c and 5.17c. If the impact forces between the journal and bearing are associated with noise, the fluid clearly acts as a filter in so far as the high frequencies or disturbances are removed or at least reduced. Similar to the case of dry contact with friction simulation, in the transition model the journal

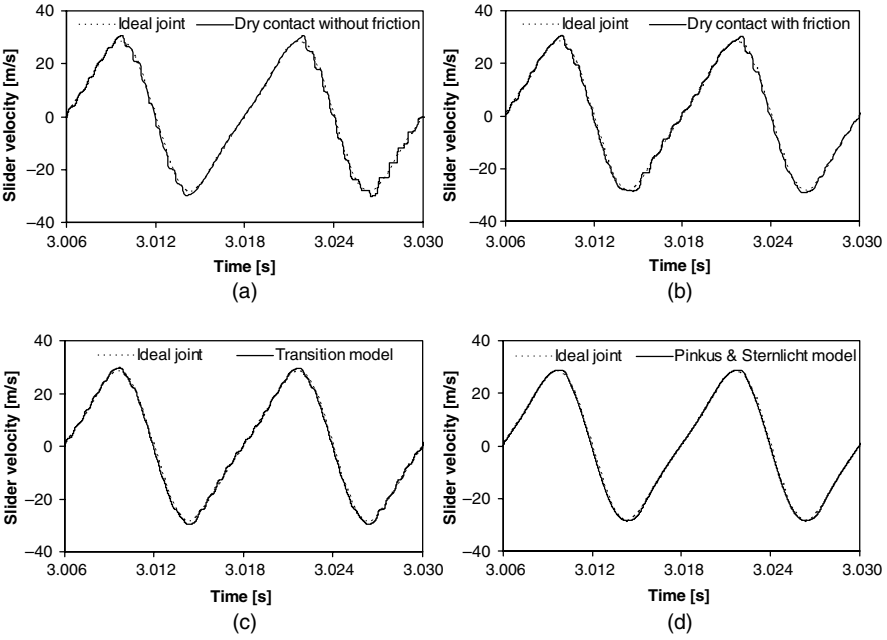

Fig. 5.15 Slider velocity: (**a**) dry contact without friction; (**b**) dry contact with friction; (**c**) transition model; (**d**) Pinkus and Sternlicht hydrodynamic model

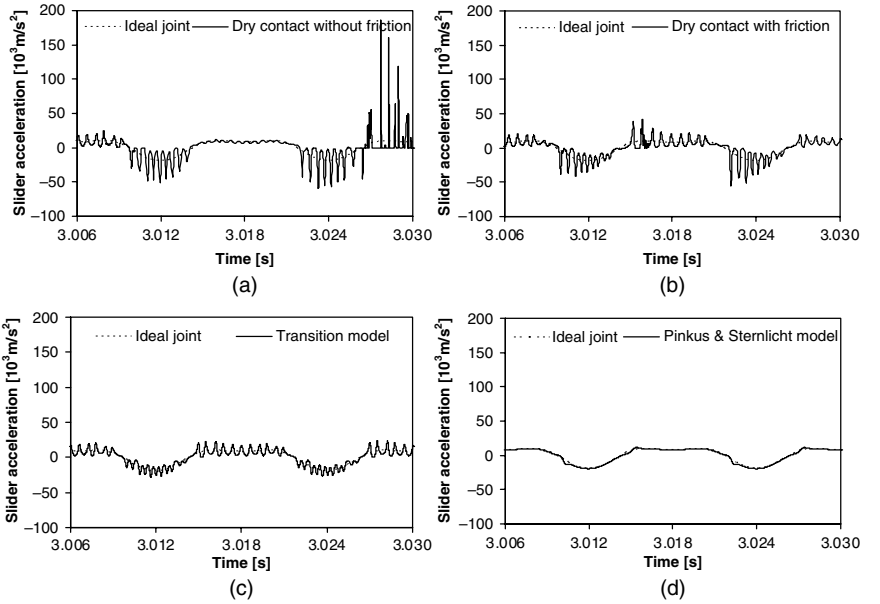

Fig. 5.16 Slider acceleration: (**a**) dry contact without friction; (**b**) dry contact with friction; (**c**) transition model; (**d**) Pinkus and Sternlicht hydrodynamic model

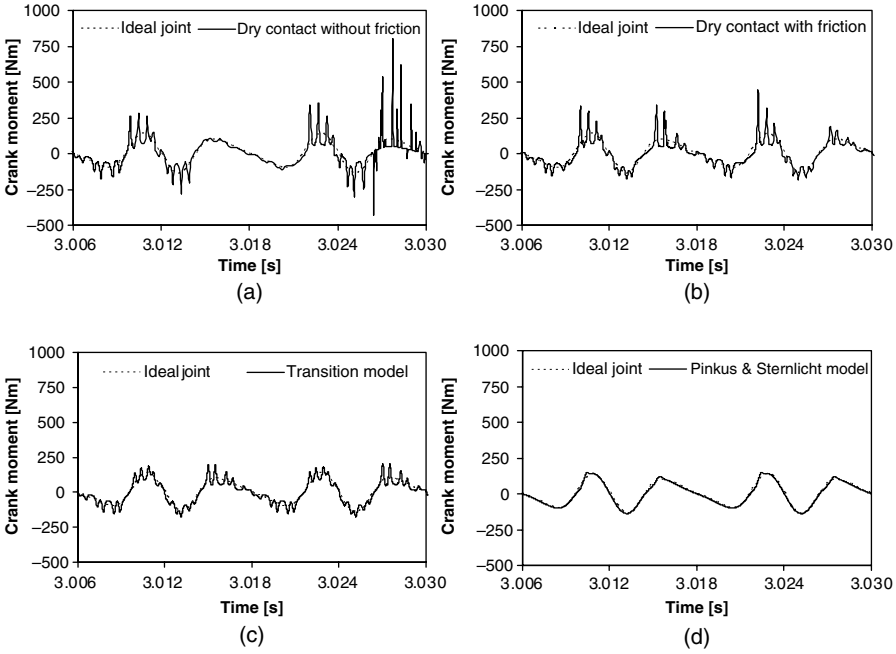

Fig. 5.17 Crank moment: (**a**) dry contact without friction; (**b**) dry contact with friction; (**c**) transition model; (**d**) Pinkus and Sternlicht hydrodynamic model

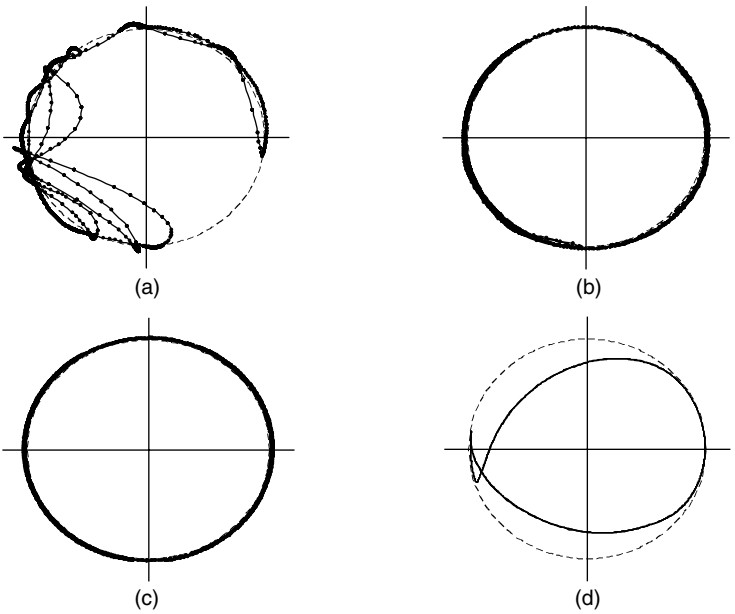

Fig. 5.18 Journal center path: (**a**) dry contact without friction; (**b**) dry contact with friction; (**c**) transition model; (**d**) Pinkus and Sternlicht hydrodynamic model

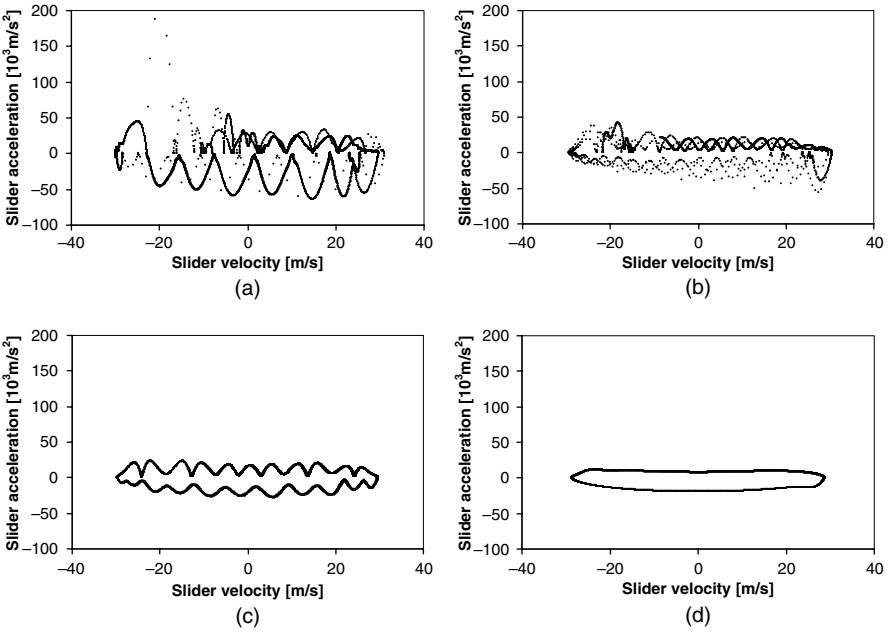

Fig. 5.19 Crank moment: (**a**) dry contact without friction; (**b**) dry contact with friction; (**c**) transition model; (**d**) Pinkus and Sternlicht hydrodynamic model

and bearing are in continuous or permanent contact during all the simulation as is visible in Fig. 5.18c. Hence the system behavior tends to be periodic, as illustrated in the corresponding Poincaré map in Fig. 5.19c.

In the case of the hydrodynamic force model given by Pinkus and Sternlicht, the overall results of the slider–crank mechanism simulation shown in Figs. 5.15d, 5.16d and 5.17d are quite close to those obtained for ideal joints. Clearly, in the case of lubricated revolute joints, the reaction forces developed are much smoother and the peak values are practically removed when compared with the unlubricated case. The system response is clearly periodic or regular, but some numerical instability is observed when the journal moves close to the bearing wall because the system becomes very stiff for a large eccentricity. In the hydrodynamic model, the fluid acts as a nonlinear spring–damper element introducing stiffness and damping to the system. This means that the lubricant absorbs part of the energy produced by the slider–crank mechanism. This is one of the main advantages for the use of fluid lubricants in the joints of machines and mechanisms. In order to better understand the efficiency and accuracy of the lubricated revolute joint using the Pinkus and Sternlicht model, the slider–crank model is considered again for another study. Table 5.3 shows the properties for the new set of study cases.

The performance of the slider–crank mechanism is quantified by plotting the reaction force produced by the fluid on the lubricated joint and the driving crank moment, displayed in Fig. 5.20a and b. In addition, the journal center orbit inside the bearing limits and the minimum oil film thickness are also plotted in Fig. 5.21a and b. The time interval used corresponds to two complete crank rotations. The results are compared to those obtained when the system is modeled with ideal joints only.

From Fig. 5.20a and b it is clear that the results are of the same order of magnitude as those obtained with ideal joints. The first and the second crank cycles show the same results which indicate that the system has reached steady-state operation conditions. This can be confirmed by the orbit of the journal center relative to the bearing center, in which the journal moves far away from the bearing wall, meaning that there is always a minimum film lubricant in between the two bodies, as shown in Fig. 5.21a and b. Since the load on the journal–bearing under consideration is not constant in direction and magnitude, the journal center describes a trajectory within the bearing boundaries as displayed in Fig. 5.21a. This means that the steady-state equilibrium is not reached, which results in a time-dependent loci of the journal center inside the bearing.

The practical criterion for determining whether or not a journal–bearing is operating satisfactorily is the value of the minimum film thickness, which is probably the most important parameter in the performance of journal–bearings.

Table 5.3 Parameters used in the simulations of the slider–crank mechanism

Bearing radius	10.0 mm
Radial clearance	0.2 mm
Journal–bearing length	40.0 mm
Oil viscosity	400 cP

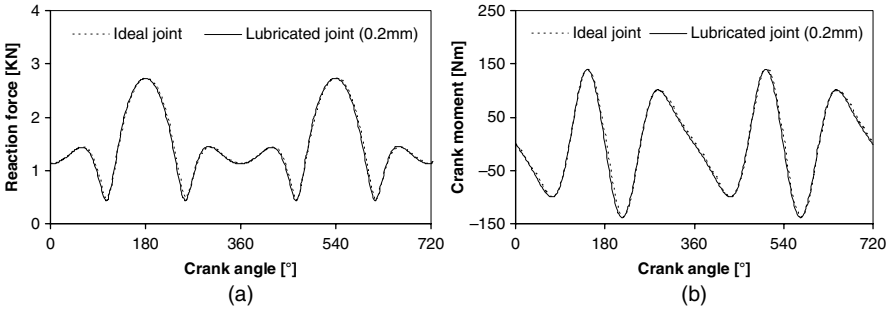

Fig. 5.20 (**a**) Reaction force developed in the lubricated revolute joint, $c = 0.2\,\mathrm{m}m$, $\mu = 400\,\mathrm{c}P$; (**b**) driving crank moment, $c = 0.2\,\mathrm{m}m$, $\mu = 400\,\mathrm{c}P$

The minimum film thickness for an aligned journal–bearing is given by

$$h_{min} = c(1 - \varepsilon) \tag{5.33}$$

where ε is the eccentricity ratio and c is the radial clearance. For safe journal–bearings performance, a minimum film thickness is required.

The safe allowable film thickness depends on the surface finish of the journal. Hamrock (1994) suggests that the safe film thickness should be greater than 2.5 μm. In practical engineering design, it is recommended that the safe film thickness should be at least 0.00015 mm/mm of bearing diameter (Phelan 1970). Similar value for the minimum film thickness can be obtained using the ESDU 84031 Tribology Series (1991) design criterion, shown in Fig. 5.22, which depends on the size of the journal–bearing.

The surface quality of the journal–bearing should be consistent with the expected film thickness and it is, therefore, usual for smaller journal–bearings to be finished to higher standards than larger journal–bearings. ESDU 84031 Tribology Series (1991) suggests that the surface roughness value of the journal–bearings should be not

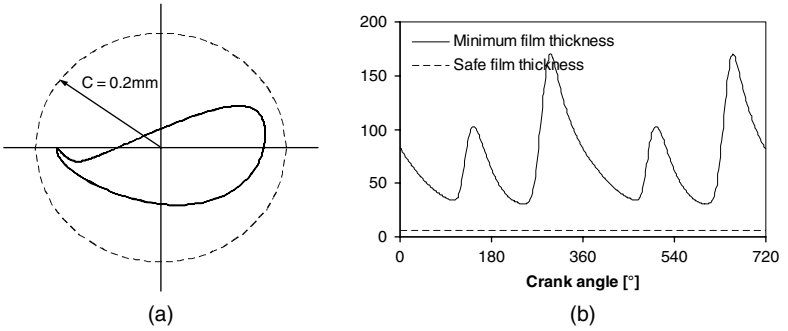

Fig. 5.21 (**a**) Journal center trajectory inside the bearing, $c = 0.2\,\mathrm{m}m$, $\mu = 400\,\mathrm{c}P$; (**b**) minimum and safe oil film thickness, $c = 0.2\,\mathrm{m}m$, $\mu = 400\,\mathrm{c}P$

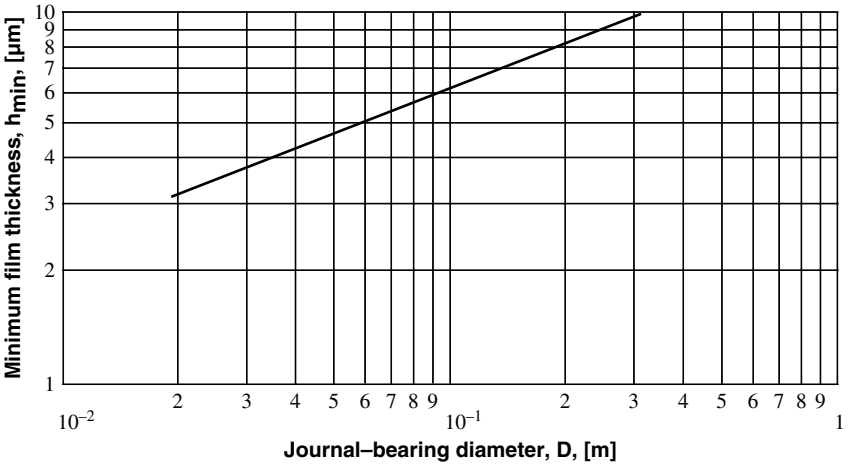

Fig. 5.22 Design chart for the minimum film thickness (adapted from ESDU 84031 Tribology Series 1991)

worse than 1/20 of the minimum film thickness. Thus for the journal–bearing considered here, the safe film thickness that ensures good operating conditions is close to 3 μm. For the present example, the film thickness is always larger than this safe film thickness as demonstrated in Fig. 5.21b.

Equations (5.14)–(5.18) show that the parameters influencing the journal–bearing performance are the oil viscosity μ, the radial clearance c, the bearing length L, the journal radius R_J and the dynamic journal–bearing parameters ω, ε, $\dot{\varepsilon}$, γ and $\dot{\gamma}$. Since the dynamic parameters of the journal–bearing depend directly on the system configuration, the radial clearance size and the oil viscosity are the only possible variables. Thus, in the following, several simulations of the slider–crank mechanism for different values of clearance size and oil viscosity are performed. The behavior of the mechanism is quantified by measuring the values of joint reaction force, driving crank moment and journal center trajectory. The values used for the radial clearance size are 0.5 and 0.1 mm, while the oil viscosity values are 400 and 40 cP.

There are some important differences between the results presented above, namely in what concerns the radial clearance size and oil viscosity influence on the joint reaction force and crank moment; such differences are graphically displayed in Figs. 5.23–5.28. The journal–bearing clearance is an important factor for the satisfactory operation of the journal–bearings. Small values of clearance can give rise to high journal–bearing temperatures while large values of clearance can mean excessive lubricant flow rates. Furthermore the results clearly show the sensitivity of the system response with different values of viscosity. As expected, with low viscosity the journal and the bearing walls are closer than with high viscosity, which suggests the possibility of metal-to-metal contact, especially visible in Figs. 5.26–5.28. Moreover there are some numerical instabilities associated with the lubricated model, namely when the oil viscosity is low, the clearance is too

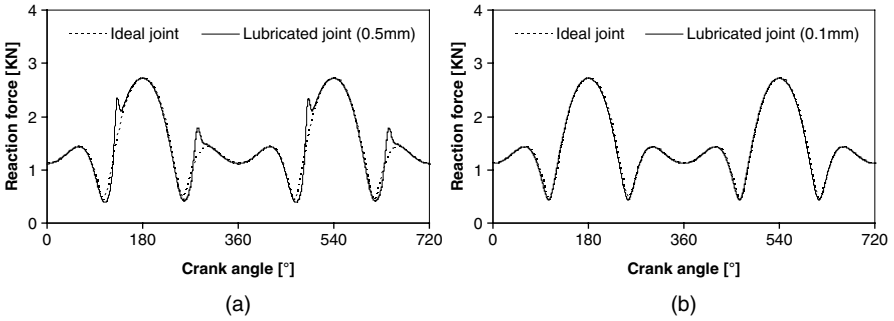

Fig. 5.23 Reaction force developed in the lubricated revolute joint: (**a**) $c = 0.5\,\mathrm{m}m$, $\mu = 400\,\mathrm{c}P$; (**b**) $c = 0.1\,\mathrm{m}m$, $\mu = 400\,\mathrm{c}P$

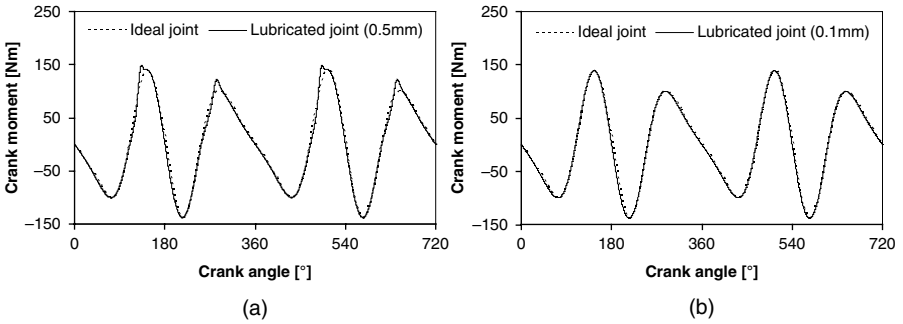

Fig. 5.24 Driving crank moment: (**a**) $c = 0.5\,\mathrm{m}m$, $\mu = 400\,\mathrm{c}P$; (**b**) $c = 0.1\,\mathrm{m}m$, $\mu = 400\,\mathrm{c}P$

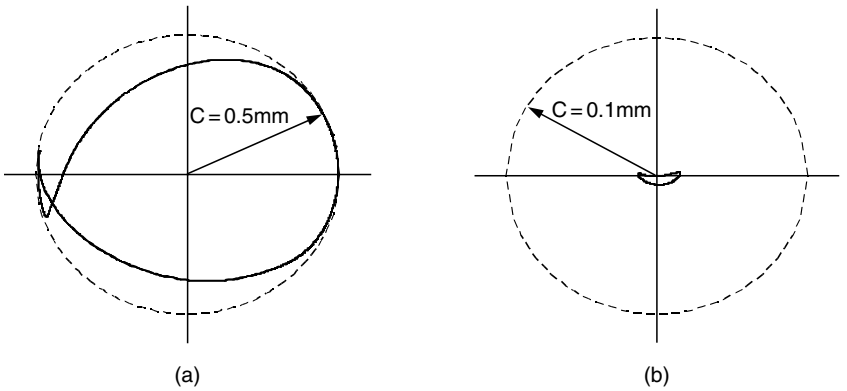

Fig. 5.25 Journal center trajectory inside the bearing: (**a**) c=0.5 mm, μ=400 cP; (**b**) c=0.1 mm, μ=400 cP

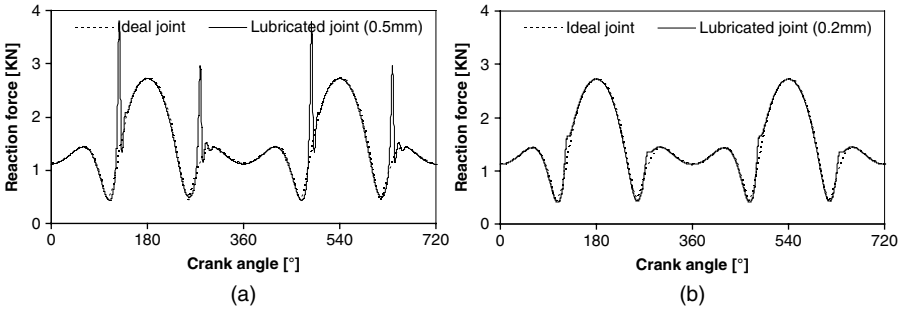

Fig. 5.26 Reaction force developed in the lubricated revolute joint: (**a**) $c = 0.5\,\mathrm{m}m$, $\mu = 40\,\mathrm{c}P$; (**b**) $c = 0.2\,\mathrm{m}m$, $\mu = 40\,\mathrm{c}P$

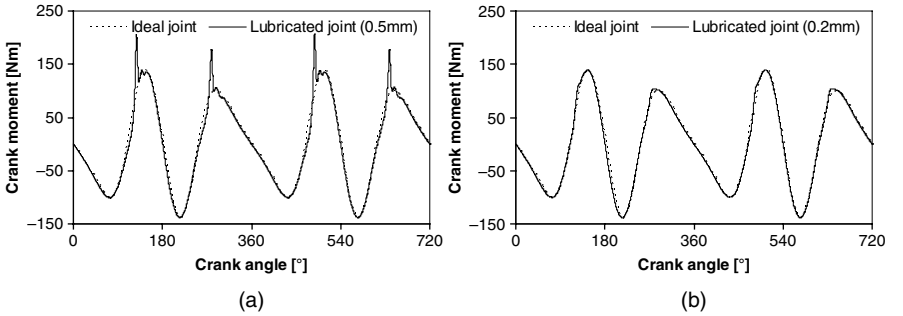

Fig. 5.27 Driving crank moment: (**a**) $c = 0.5\,\mathrm{m}m$, $\mu = 40\,\mathrm{c}P$; (**b**) $c = 0.2\,\mathrm{m}m$, $\mu = 40\,\mathrm{c}P$

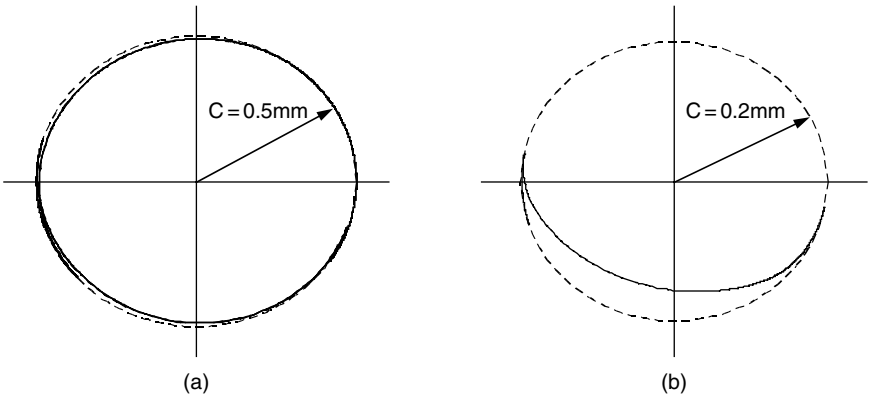

Fig. 5.28 Journal center trajectory inside the bearing: (**a**) $c = 0.5\,\mathrm{m}m$, $\mu = 40\,\mathrm{c}P$; (**b**) $c = 0.2\,\mathrm{m}m$, $\mu = 40\,\mathrm{c}P$

large or for a combination of these two factors. These numerical difficulties are well represented by some peaks in the joint reaction force and crank moment diagrams, because the journal and bearing walls are very close to each other. On the other hand, when the two elements are very close, the hydrodynamic lubrication theory is no longer valid and the EHL theory must be taken into account (Rahnejat 2000).

5.8 Summary

A comprehensive methodology for modeling lubricated revolute joints in multibody mechanical systems was presented in this chapter. A simple journal–bearing and the slider–crank mechanism were chosen as demonstrative examples of the application of the techniques used. Furthermore a parametric study of the slider–crank mechanism for different values of clearance size and oil viscosity was performed in order to provide the results necessary for the comprehensive discussion of the models proposed.

For dynamically loaded journal–bearings, the classic analysis problem consists in predicting the motion of the journal center under arbitrary and known loading. On the contrary, in the present analysis the time-variable parameters are known from the dynamic analysis and the instantaneous force on the journal–bearing is calculated on the bodies of the models proposed. The forces built up by the lubricant fluid are evaluated from the state of variables of the system and included in the equations of motion.

Both squeeze and wedge hydrodynamic effects are included in the analysis of dynamically loaded journal–bearings. It should be mentioned that the methodology presented here uses the superposition principle of wedge effect entrainment and squeeze-film effect to calculate the load capacity. This is only approximate and has been adopted in the work in order to lead to an analytic solution, rather than to a purely numerical one. Furthermore the methodology is only applicable to long bearings, which is seldom the case in most engine bearings, but it can be useful for many other mechanisms. This is the compromise used here for the sake of computational efficiency.

In an application for a slider–crank mechanism, for instance, the reaction moment necessary to drive the crank with a constant angular velocity is of the same order of magnitude as the one in the case of an ideal joint, meaning that the global motion of the slider–crank mechanism with a lubricated joint is periodic or regular. The lubricant acts as a nonlinear spring–damper in so far as lubricated journal–bearing absorbs some of the energy produced by the slider when it accelerates or decelerates, which results in lower reaction moment compared to ideal joints. The lubricant introduces effective stiffness and damping to the slider–crank mechanism. Therefore a hydrodynamic fluid film journal–bearing exhibits a damping effect that plays an important role in the stability of the mechanical components.

The transition model that takes into account the existence of the lubricant during the free flight of the journal and the possibility for dry contact under some conditions

seems to be well fitted to describe joints with clearances. The similarity of the forces is notable in the transition model when compared with those of the EHL theory.

The minimum film thickness is a fundamental parameter in the study of a hydrodynamic journal–bearing. The value of the minimum oil film thickness defines the kind of regime of lubrication which is present in the journal–bearing, namely thick-film lubrication, where the journal–bearing surfaces are totally separated by the lubricant and thin-film lubrication in which the field of pressure developed produces elastic deformation. The lubrication between two moving surfaces can shift between these two regimes, depending on the velocity, lubricant viscosity and roughness of surfaces.

The viscosity, which is associated with the resistance to the flow, is one of the most important properties of the fluid lubricants employed in journal–bearings. Actually the behavior of the journal–bearings is quite sensitive to the oil viscosity. As expected, with low working viscosity, the journal and the bearing walls are closer than with high viscosity, which can lead to the possibility of metal-to-metal contact. With higher viscosity there are higher reaction moments produced in systems. This is due to the fact that the lubricant becomes more rigid and absorbs less energy from the system. Moreover the fluid film in conventional journal–bearings can reach a very small thickness and the pressure gradient generated under some conditions can produce elastic deformations of the same order of the magnitude of the film thickness. Thus for a rigorous analysis the elastic deformation must also be considered.

The clearance size also has an important effect on the performance of the journal–bearings. Higher clearance leads to a larger space for the lubricant to flow. The position of the journal loci moves within the bearing, so there is less pressure produced, the motion of the journal being a result of that. Also lower clearance means higher hydrodynamic forces, higher system rigidity and consequently higher reaction forces on the system. Lower clearance produces fewer fluctuations due to the increased damping, which means less vibration and instability problems.

The quantitative solutions for lubricated journal–bearings in mechanical systems presented in this chapter are quite useful in so far as they are given in a closed form. The hydrodynamic model for lubricated revolute joints in mechanical systems is numerically efficient and fast because the pressure distribution does not need to be evaluated. Furthermore the methodology is easy and straightforward to implement in a computational code because resultant forces due to the fluid action are obtained in explicit form. Some numerical difficulties can be observed when either the fluid viscosity is too low or the radial clearance of the journal–bearing is too large, which leads to large eccentricities and, consequently, the system becomes stiff.

References

Alshaer BJ, Lankarani HM (2001) Formulation of dynamic loads generated by lubricated journal bearings. Proceedings of DETC'01, ASME 2001 design engineering technical conferences and computers and information in engineering conference, Pittsburg, PA, September 9–12, 8pp.

Bauchau OA, Rodriguez J (2002) Modelling of joints with clearance in flexible multibody systems. International Journal of Solids and Structures 39:41–63.

Boker JF (1965) Dynamically loaded journal bearings: mobility method of solution. Journal of Basic Engineering 4:537–546.
Claro JCP (1994) Reformulação de método de cálculo de chumaceiras radiais hidrodinâmicas—análise do desempenho considerando condições de alimentação. Ph.D. Dissertation, University of Minho, Guimarães, Portugal.
Costa LAM (2000) Análise do desempenho de chumaceiras radiais hidrodinâmicas considerando efeitos térmicos. Ph.D. Dissertation, University of Minho, Guimarães, Portugal.
Dowson D, Taylor CM (1979) Cavitation in bearings. Annual review of fluid mechanics, edited by JV VanDyke et al., Vol. 11, pp. 35–66. Annual Reviews Inc., Palo Alto, CA.
Dubois GB, Ocvirk FW (1953) Analytical derivation and experimental evaluation of short-bearing approximation for full journal bearings, NACA Rep. 1157.
Elrod HG (1981) A cavitation algorithm. Journal of Lubrication Technology 103:350–354.
ESDU 84031 Tribology Series (1991) Calculation methods for steadily loaded axial groove hydrodynamic journal bearings. Engineering Sciences Data Unit, London, England.
Flores P, Ambrósio J (2004) Revolute joints with clearance in multibody systems. Computers and Structures, Special Issue: Computational Mechanics in Portugal 82(17–18):1359–1369.
Frêne J, Nicolas D, Degneurce B, Berthe D, Godet M (1997) Hydrodynamic lubrication—bearings and thrust bearings. Elsevier, Amsterdam, The Netherlands.
Goenka PK (1984) Analytical curve fits for solution parameters of dynamically loaded journal bearings. Journal of Tribology 106:421–428.
Hamrock BJ (1994) Fundamentals of fluid film lubrication. McGraw-Hill, New York.
Miranda AAS (1983) Oil flow, cavitation and film reformulation in journal bearings including interactive computer-aided design study. Ph.D. Dissertation, Department of Mechanical Engineering, University of Leeds, United Kingdom.
Mistry K, Biswas S, Athre K (1997) A new theoretical model for analysis of the fluid film in the cavitation zone of a journal bearing. Journal of Tribology 119:741–746.
Nikravesh PE (1988) Computer-aided analysis of mechanical systems. Prentice Hall, Englewood Cliffs, NJ.
Phelan RM (1970) Fundamentals of mechanical design, Third edition. McGraw-Hill, New York.
Pinkus O, Sternlicht SA (1961) Theory of hydrodynamic lubrication. McGraw-Hill, New York.
Rahnejat H (2000) Multi-body dynamics: historical evolution and application. Proceedings of the Institution of Mechanical Engineers, Journal of Mechanical Engineering Science 214(C):149–173.
Ravn P (1998) A continuous analysis method for planar multibody systems with joint clearance. Multibody System Dynamics 2:1–24.
Ravn P, Shivaswamy S, Alshaer BJ, Lankarani HM (2000) Joint clearances with lubricated long bearings in multibody mechanical systems. Journal of Mechanical Design 122:484–488.
Sommerfeld A (1904) Zur hydrodynamischen theorie der schmiermittelreibung. Zeitschrift für Angewandte Mathematik und Physik 50:97–155.
Woods CM, Brewe DE (1989) The solution of the Elrod algorithm for a dynamically loaded journal bearing using multigrid techniques. Journal of Tribology 111:302–308.